PHYSOR 2018: Reactor Physics paving the way towards more efficient systems
Cancun, Mexico, April 22-26, 2018

COMPARISON OF NEUTRONICS PERFORMANCE CHARACTERISTICS OF THE PROPOSED NIST REACTOR WITH DIFFERENT LEU FUELS

Danyal J. Turkoglu[1], Zeyun Wu[2], Robert E. Williams[1] and Thomas H. Newton[1]

[1]NIST Center for Neutron Research
100 Bureau Drive, Mail Stop 6101, Gaithersburg, MD 20899 USA

[2]Department of Mechanical and Nuclear Engineering
Virginia Commonwealth University, Richmond, VA 23219 USA

danyal.turkoglu@nist.gov, zwu@vcu.edu, robert.williams@nist.gov, thomas.newton@nist.gov

ABSTRACT

As a potential replacement for the NBSR, a conceptual design of a new reactor with a horizontally-split core using low-enriched uranium silicide dispersion (U_3Si_2/Al) fuel has recently been studied. In this paper, the neutronics calculations with low-enriched UMo fuels (monolithic U10Mo and U7Mo/Al dispersion) and U_3Si_2/Al fuel are compared with the objective of identifying the best fuel candidate for the reactor for practical operations and maximum cold neutron production. For the comparisons, fuel inventories for multi-cycle equilibrium cores were calculated for each fuel based on a 30 day reactor cycle at 20 MW power. With its very high U density, the potential to load more U in the core with U10Mo monolithic fuel was explored with test cases using an alternate fuel management scheme, a higher power level (30 MW), or a longer cycle (45 days).

KEYWORDS: Low-Enriched Uranium, Research Reactor, Neutronics Performance Characteristics

1. INTRODUCTION

A conceptual design of a reactor, referred to as the NBSR-2 in this paper, is being studied as a potential replacement for the NBSR [1], which has operated for over 50 years at the National Institute of Standards and Technology (NIST) Center for Neutron Research (NCNR). Feasibility studies have demonstrated the potential for the NBSR-2 design to provide bright cold neutron beams for scientific experiments [2, 3]. The proposed design, with 20 MW thermal power and a 30 day operating cycle, was selected to be on a similar scale as the NBSR. For improved neutron flux performance, the design consists of a horizontally-split compact core that is cooled and moderated by light water while reflected by heavy water [4]. The fuel elements (FEs) in the design are conventional plate type for test reactors using low-enriched uranium (LEU) with ^{235}U enrichments less than 20 % by weight to comply with nuclear non-proliferation requirements. U_3Si_2/Al dispersion fuel was chosen for initial studies to investigate and verify the viability of the novel design in terms of neutronics and safety performance characteristics [3].

U_3Si_2/Al dispersion fuel was prioritized for the initial NBSR-2 studies because it has the highest U density (4.8 g/cm^3) out of the LEU fuels qualified by the US Nuclear Regulatory Commission for use in research and test reactors. However, the U_3Si_2/Al dispersion fuel is not being considered as the fuel for five high performance research reactors (HPRRs) in the United States, including the NBSR, following their conversion from high-enriched uranium (HEU) to LEU fuel. There are a couple of reasons for seeking alternative fuels. First, U_3Si_2/Al fuel has a relatively-low ^{235}U density, which makes it difficult to achieve high power densities. Second, the power density with U_3Si_2/Al dispersion fuel in HPRRs must be limited to comply with the current regulatory limit that the peak heat flux be less than 140 W/cm^2 [5].

LEU fuels containing high-density uranium molybdenum (UMo) alloys are being developed for use in HPRRs [6] to address their fuel requirements. While the fuel conversion program in the United States is focused on U10Mo monolithic fuel [7], UMo dispersion fuels are being pursued in other countries [8, 9]. In this paper, these advanced LEU fuels, the UMo monolithic and dispersion fuels, were modeled in the current NBSR-2 design with the resulting neutronics performance characteristics compared with the U_3Si_2/Al dispersion fuel as a reference for their performances. Thermal hydraulics, safety analyses, and engineering constraints were not evaluated in this study.

2. LEU FUELS FOR HIGH PERFORMANCE RESEARCH REACTORS

The NBSR-2 is a "tank-in-pool" design with an Al tank (2 m height and 2 m diameter) that is filled with heavy water and is placed in a pool of light water. The heavy water in the tank is the reflector for the core, while the core itself is moderated and cooled by light water. The core is split horizontally to maximize the useful flux trap volume between the two halves. Each half contains nine fuel elements in a Zr box that is the boundary between light water and heavy water. Two cold neutron sources (CNSs), not yet optimized in design, are placed 40 cm from the reactor on the north and south sides of the flux trap. The positions of the CNSs balance a tradeoff between cold neutron performance and estimated heat load for the CNSs. Four '#' shaped hafnium control blades provide criticality and safety control. Schematics of the NBSR-2 are shown in Figure 1. A complete description of the NBSR-2 design can be found in Ref [3].

The NBSR-2 was fueled in previous studies with 18 fuel elements each containing 17 plates of U_3Si_2/Al dispersion fuel. U_3Si_2/Al dispersion fuel was qualified for U densities up to 4.8 g/cm^3. Two UMo fuels, with higher U densities than U_3Si_2/Al, are considered in this work: U7Mo/Al dispersion fuel and U10Mo monolithic fuel, which have Mo mass fractions of 7 % and 10 %, respectively. The U10Mo monolithic fuel is a pure metallic alloy that has a very high U density of 15.5 g/cm^3. Table I summarizes the three LEU fuels investigated in this paper.

Table I: Comparison of the three LEU fuels.

Fuel	**U_3Si_2/Al**	**U7Mo/Al**	**U10Mo**
Type	Dispersion	Dispersion	Monolithic
Compositions	U, Si, Al	U, Mo, Al	U, Mo
Enrichment (%)	19.75	19.75	19.75
Density (g/cm^3)	6.52	9.97	17.22
Uranium density (g/cm^3)	4.80	7.98	15.50
U-235 density (g/cm^3)	0.95	1.58	3.06

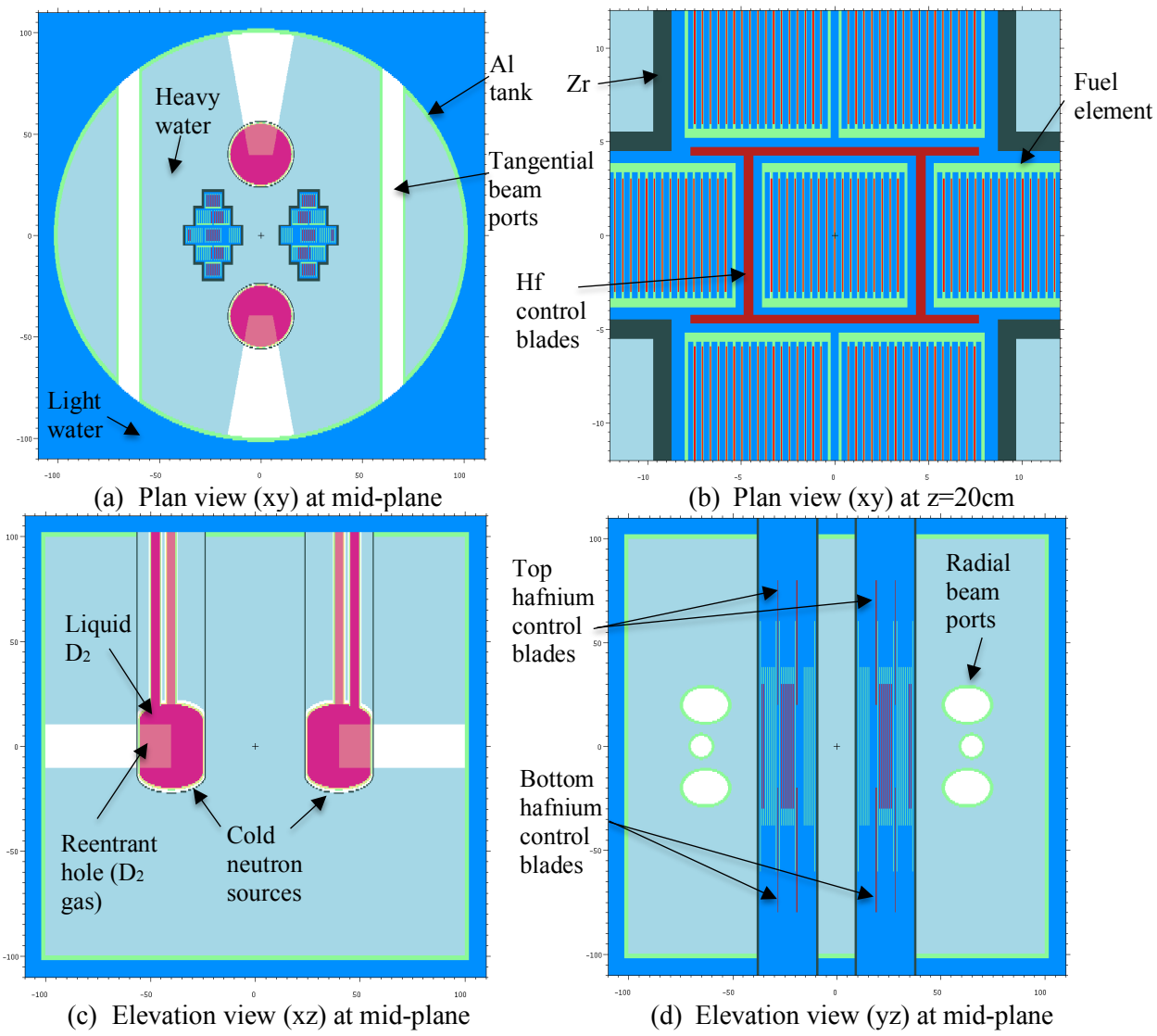

Figure 1. Schematics of the NBSR-2.

Reactions of UMo alloy with Al cladding and Al powder (in the dispersion fuel) cause the formation of interaction layers that, along with other effects such as recrystallization [10], lead to fuel swelling at high burnups. To mitigate these adverse effects and prevent delamination in the case of U10Mo monolithic fuel, a protective interlayer of Zr is added between the U10Mo foil and the Al cladding [11]. The reference U10Mo fuel system uses a 25.4 μm thick (1 mil) layer of Zr. For UMo dispersion fuel, the addition of Si to the dispersion has been found to reduce the interaction layers [12] and mitigate fuel swelling for fission densities > 3.0×10^{21} cm^{-3} [13], but is neglected in this study.

The dimensions of the fuel meat can be adjusted to some extent by the designer in the model to achieve specific goals. In this study, an initial point for the LEU fuel designs was to vary the fuel meat thickness to achieve a similar mass of ^{235}U in each fuel plate. The three LEU fuels were modeled with 17-plate fuel elements having a constant fuel plate thickness (50 mil), as shown in Figure 2, to keep the water channel thickness constant for the purpose of comparison. The parameters of the UMo fuels in this study are similar to those used in the preliminary analyses for the conversion of NBSR from HEU to LEU [14, 15].

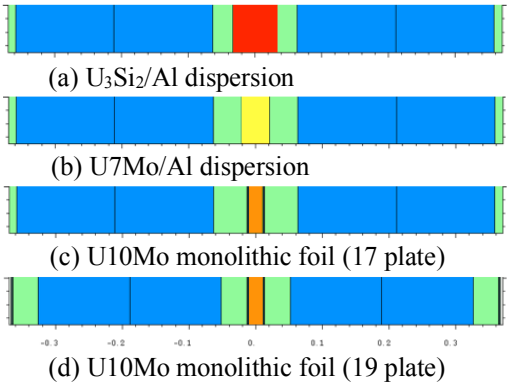

Material	Color
Light water	
Aluminum cladding	
U_3Si_2/Al dispersion	
U7Mo/Al dispersion	
U10Mo monolithic foil	
Zr interlayer	

Figure 2. The cross-sectional views of the three LEU fuels being investigated.

For the U10Mo fuel, the cladding thickness can be substantially reduced since the fuel meat is very thin, opening the possibility for 19 fuel plates in each element. The higher U loading with 19-plate fuel elements in the core presents the opportunity to: 1) extend the reactor cycle beyond 30 days, 2) extend burnup of fuel elements by burning them for more than three cycles, and/or 3) operate at higher thermal power. Thus, a model with 19-plate fuel elements was created for the U10Mo case to explore these options. The parameters for three LEU fuels studied in this paper are summarized in Table II.

Table II: Fuel parameters of the LEU Fuels.

Parameter	U_3Si_2/Al	U7Mo/Al	U10Mo (17[a])	U10Mo (19[a])
Number of plates per FE	17	17	17	19
Coolant channel width (cm)	0.295	0.295	0.295	0.275
Fuel meat length (cm)	60	60	60	60
Fuel meat width (cm)	6.134	6.134	6.134	6.134
Fuel meat thickness (mil)	26.0	16.2	8.5 (10.5[b])	8.5 (10.5[b])
Fuel plate thickness (mil)	50	50	50	42.5
Cladding thickness (mil)	12	17	19.75	16
Fuel meat volume (cm^3)	24.31	15.14	7.95	7.95
Fuel meat mass (g)	158.48	151.22	136.83	136.83
Total U-235 mass in FE (g)	392.5	406.7	413.6	462.2

[a] The number in parenthesis refers to the number of plates in each FE
[b] Including the 1 mil Zr interlayer on both sides of the foil

3. RESEARCH METHODOLOGIES

The neutronics calculations were performed using MCNP6, a generalized Monte Carlo code for radiation transport. Key performance characteristics of the core, such as neutron flux and fission rate, can be calculated by MCNP6 with multi-cycle equilibrium core. To consistently obtain the fuel inventories of the multi-cycle equilibrium cores for the three LEU fuels, a process was developed based on an iterative equilibrium core search procedure [16]. Starting from a core of fresh fuel elements, the criticality calculation (KCODE) and depletion/burnup (BURN) features of MCNP6 were used to simulate six reactor

cycles in an iterative process. Each cycle was split into four stages: startup (SU) for 1.5 days to achieve equilibrium ^{135}Xe, beginning of cycle (BOC), middle of cycle (MOC), and end of cycle (EOC).

The fuel elements were shuffled according to one of the two fuel management schemes shown in Figure 3. In Scheme A, the first number in the pair denotes the fuel batch number and the second number is unique identifier for the FE in the batch. In Scheme B, the first number denotes the batch number and the second number denotes the number of cycles that the element will go through. In both cases, the black and white font colors distinguish FEs in the separate cores.

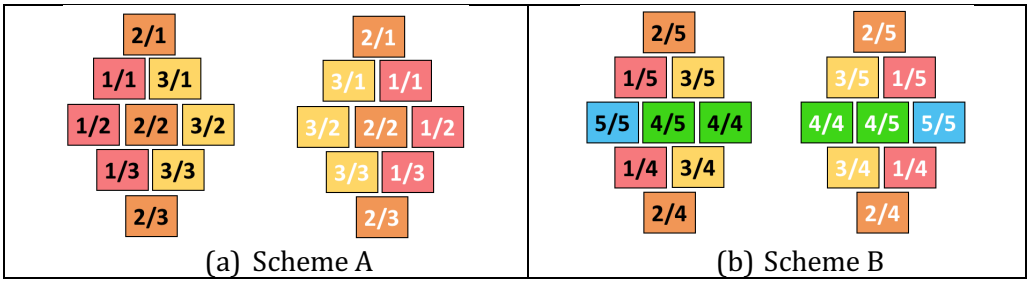

Figure 3. The fuel management schemes used in this study.

In Scheme A, six fresh fuel elements are added each cycle, and the six third-cycle fuel elements are discarded at the end of cycle. Scheme B uses only four fresh fuel elements each cycle, with two fourth-cycle fuel elements and two fifth-cycle elements discarded at the end of cycle. Scheme A was used for all cases except for a case with 19-plate U10Mo fuel elements. The fuel materials for each element was discretized into six axial zones.

Figure 4 shows the flow diagram for the equilibrium core search process that was fully automated with a Python script for consistent application to the different cases being investigated. The process began with a core of fresh fuel elements. With the SU model, the control blade worth curve was determined in order to estimate control blade positions to achieve keff of 1.01 based on the excess reactivity in the core. Following the adjustment of control blades, an updated input with the BURN card was run for the designated length to calculate the fuel depletion and fission product inventories. The fuel elements decayed for 7 days following MOC and were reloaded based on the fuel management scheme. Six cycles were simulated for each case.

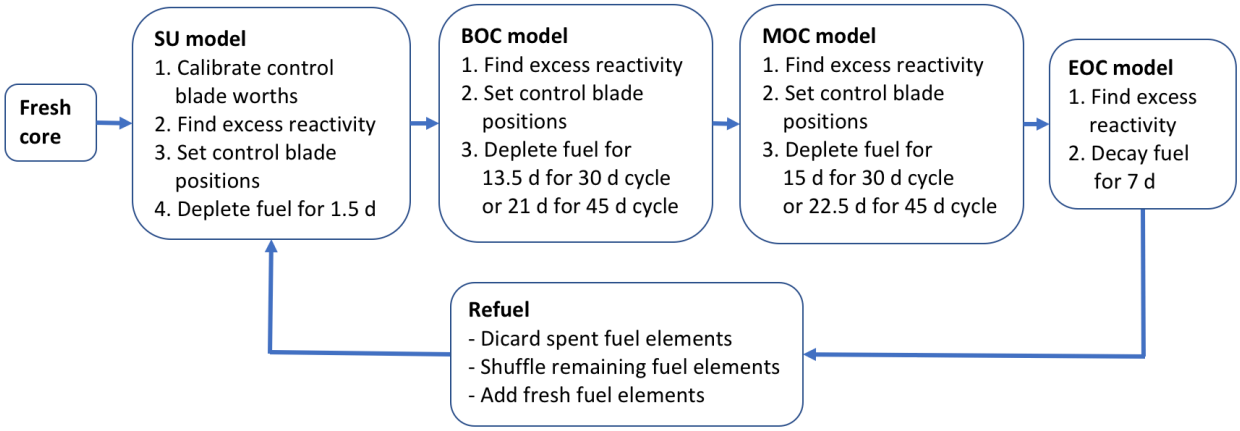

Figure 4. The iterative process with MCNP6 for finding fuel inventories of the equilibrium core

4. RESULTS

After estimating the equilibrium core models for each LEU fuel, the fuel inventories and CNS performances were compared.

4.1. Excess reactivity

Although the different LEU fuel elements contain similar ^{235}U masses in the 17-plate model, slight differences in the power distribution and neutron economy can affect the fuel burnup, and, therefore, the maximum cycle length at a given power. Analyzing the results from the equilibrium core search, the excess reactivities ($\Delta\rho = \frac{k_{eff}-1}{k_{eff}}$) at the beginning of the SU, MOC and EOC stages, shown in Figure 5(a), indicate that the LEU fuels in the 17-plate model perform similarly with the given power level, fuel management scheme and cycle length. Figure 5(b) shows the results for excess reactivity for the 19-plate model with U10Mo fuel using (Case 1) Scheme A with a 30 day cycle length at 30 MW, (Case 2) Scheme B with a 45 day cycle length at 20 MW and (Case 3) Scheme B with a 30 day cycle length at 20 MW. Based on these results for U10Mo fuel, the excess reactivity in the 19-plate model was sufficient for 900 MW-days (MWD) of operation in (Case 1) and (Case 2) with Scheme A, as well as with (Case 3) with the hybrid 4/5 batch fuel management scheme (Scheme B).

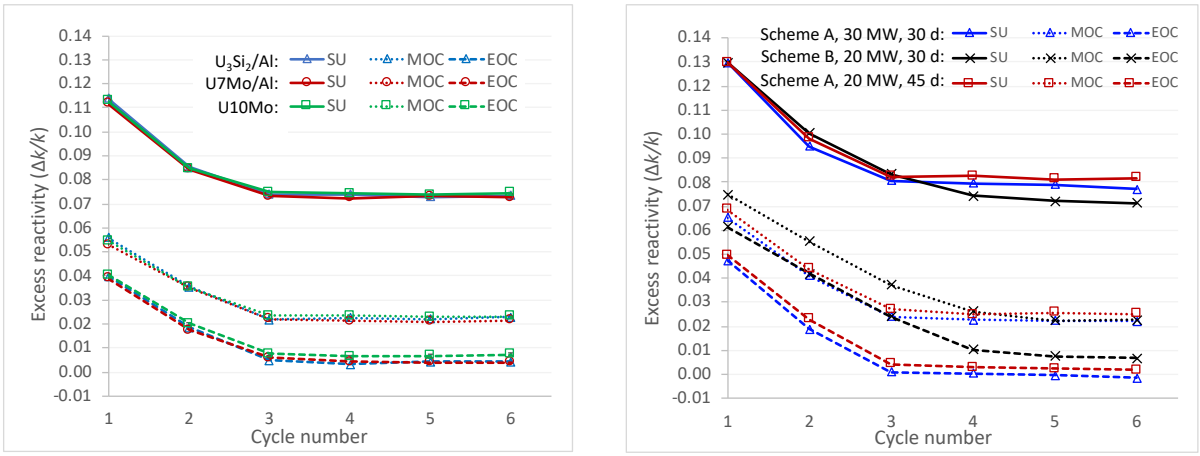

(a) 17-plate model (b) 19-plate U10Mo model

Figure 5. Excess reactivities at SU, MOC and EOC with control blades fully withdrawn (a) for the 17-plate models using the three LEU fuels and (b) for the 19-plate U10Mo models.

The fissile content of the discharged FEs at EOC of Cycle 6 in terms of ^{235}U burnup and ^{239}Pu mass for the different fuels and cycle parameters were compared, as shown in Table III. The fissile inventories of the three LEU fuels in the 17-plate model were similar, with small differences owing to the initial loading of ^{235}U. The ^{235}U burnup for the 19-plate models of the U10Mo fuel was significantly higher than the 17-plate models. The fissile inventories were similar despite differences in power and cycle length since the amount of MWD was constant. Scheme B, with only four fresh elements at SU instead of six, had discharged elements with similar burnups despite only operating for 600 MWD.

Table III: Fuel burnup and ^{239}Pu mass for the discharged elements in the west core in Cycle 6.

						^{235}U Burnup (%)			^{239}Pu mass (g)		
Fuel	**# of fuel plates**	**Fuel scheme**	**Power (MW)**	**Cycle length (days)**	**MWD**	**FE 3/1**	**FE 3/2**	**FE 3/3**	**FE 3/1**	**FE 3/2**	**FE 3/3**
U_3Si_2/Al	17	A	20	30	600	29.9	33.0	30.0	7.0	7.2	7.0
U7Mo/Al	17	A	20	30	600	28.9	31.8	29.0	7.2	7.4	7.1
U10Mo	17	A	20	30	600	28.2	31.2	28.4	7.2	7.5	7.3
	19	A	30	30	900	38.0	41.1	37.8	10.0	10.3	10.1
	19	A	20	45	900	37.3	40.1	37.1	9.9	10.0	9.8
						FE 4/4	**FE 5/5**		**FE 4/4**	**FE 5/5**	
	19	B	20	30	600	36.1	41.6		9.3	10.4	

4.2 Cold neutron source (CNS) performance

Since the primary purpose of the NBSR-2 is the production of high-intensity cold neutron beams, the CNS performance for each case was evaluated in terms of currents of cold (< 5 meV), thermal (5 meV to 0.625 eV) and fast neutrons (> 0.625 eV) at the surface of the north CNS exit hole. The power distribution, particularly the peaking at the center of the reactor, changes based on fuel burnup and control blade position, which can diminish the cold neutron flux by up to 10 % from SU to EOC. For this evaluation, the BOC model from Cycle 6 for each case was used. The control blade inserted length was set to 10 cm for each of the four control blades. The tally results were normalized by k_{eff}, which was close to unity for each case. Additionally, the CNS heat load was calculated with MCNP6 based on neutron, gamma-ray and beta particle heat loads in the deuterium, helium and Al cells; a detailed description of the heat load calculation for a CNS source can be found in Ref [17]. Table IV shows the results for neutron currents and head loads.

Table IV CNS performance in terms of neutron current and heat load.

	# of			Cycle		CNS current* ($\times 10^{11}$ n/cm^2)				CNS heat
Fuel	**fuel plates**	**Fuel scheme**	**Power (MW)**	**length (days)**	k_{eff}	**Cold**	**Thermal**	**Fast**	**Total**	**load (kW)**
U_3Si_2/Al	17	A	20	30	1.000	5.4	9.8	2.2	17.5	3.7
U7Mo/Al	17	A	20	30	0.999	5.4	9.8	2.2	17.5	3.7
U10Mo	17	A	20	30	1.001	5.4	9.7	2.2	17.3	3.7
	19	A	30	30	1.007	7.8	14.2	3.3	25.2	5.4
	19	A	20	45	1.010	5.3	9.3	2.1	16.6	3.6
	19	B	20	30	1.000	5.3	9.7	2.2	17.3	3.7
NBSR						0.89				

*All tallies were performed with cos θ greater than 0.99, where θ is the angle between the neutron streaming direction and the normal direction of the exit surface. The relative errors of the tallies are all less than 0.1%.

The CNS performances for all cases at 20 MW were similar. Increasing the power level to 30 MW offers, not surprisingly, a 50 % gain in CNS surface current – but at the expense of a proportional increase in CNS heat load to 5.4 kW. As has been demonstrated in previous studies, the NBSR-2 design outperforms the

NBSR liquid H_2 cold source in cold neutron production by more than a factor of 6 – potentially by a factor of 9 if power is increased to 30 MW. In aggregate of the cases, the NBSR-2 design has an excellent ratio of about 6 slow neutrons per fast neutron – a metric that is important for signal-to-background ratios of scientific instruments using neutron beams.

5. SUMMARY

Three LEU fuel options – U_3Si_2/Al dispersion, monolithic U10Mo and U7Mo/Al dispersion – performed similarly in 17-plate FE models that kept plate thickness constant and contained similar masses of ^{235}U in fresh FEs. The U10Mo model has a very thin fuel meat (10.5 mil) that could enable more plates in a fuel element of fixed size. We explored this possibility with a 19-plate fuel element with combinations of power levels (20 MW or 30 MW) and cycle lengths (30 days or 45 days) to demonstrate that the reactor design could potentially reach 900 MWD of operation with six fresh fuel elements per cycle. A fuel management scheme with only four fresh fuel elements, potentially lowering the operating costs, was found suitable for 600 MWD of operation in this study. However, increasing the neutron flux by 50 % for cold neutron instruments – if allowed by fuel qualification and engineering constraints that have not been explored – or extending reactor cycle to 45 days with the 19-plate U10Mo FEs could also be desirable improvements of this reactor design. In comparing the three LEU fuels, the ability to load more fuel in the NBSR-2 design with U10Mo allows more flexibility in the reactor design and could lead to other optimizations that maximize cold neutron production for scientific research at the NCNR.

REFERENCES

1. NIST, Safety Analysis Report (SAR) for License Renewal of the National Institute of Standards and Technology Reactor–NBSR; NBSR-14, Rev. 4." *National Institute of Standards and Technology* (2010)
2. Z. Wu and R.E. Williams, "Core design studies on a low-enriched uranium reactor for cold neutron sources at NIST," PHYSOR 2016, Sun Valley, ID, May1-5, 1583–1592 (2016)
3. Z. Wu, R.E. Williams, J.M. Rowe, et al, "Neutronics and Safety Studies on a Research Reactor Concept for an Advanced Neutron Source," *Nuclear Technology*, **199**, 67–82 (2017)
4. Z. Wu, M. Carlson, R.E. Williams, J.M. RoweM A Novel Compact Core Design for Beam Tube Research Reactors. *Transactions of the American Nuclear Society* **112**, 8–11 (2015).
5. "Safety Evaluation Report related to the Evaluation of Uranium Silicide-Aluminum Dispersion Fuel for Use in Non-Power Reactors", *U.S. Nuclear Regulatory Commission,* (1988)
6. J.L. Snelgrove, G.L. Hofman, M.K. Meyer, et al, "Development of very-high-density low-enriched-uranium fuels," *Nuclear Engineering and Design*, **178**, 119–126 (1997)
7. N.E. Woolstenhulme, J.I. Cole, I. Glagolenko, et al, "Irradiation Tests Supporting LEU Conversion of Very High Power Research Reactors in the US," No. INL/CON-16-39776, *Idaho National Laboratory*, Idaho Falls, ID (United States), 2016.
8. A. Leenaers, S. van den Berghe, E. Koonen, et al, "Post-irradiation examination of uranium – 7 wt % molybdenum atomized dispersion fuel," *Journal of Nuclear Materials, **335***, 39–47 (2004)
9. H.J. Ryu, J.M. Park, Y.J. Jeong, et al, "Post-irradiation analyses of U-Mo Dispersion Fuel Rods of KOMO Tests," *Nuclear Engineering Technology*, **45**, 847–858 (2013)
10. Y. Soo, G.L. Hofman, J.S. Cheon, "Recrystallization and fission-gas-bubble swelling of U – Mo fuel," *Journal of Nuclear Materials,* **436**, 14–22 (2013)
11. Robinson AB, Chang GS, Keiser DD (2009) Irradiation Performance of U-Mo Alloy Based " Monolithic " Plate-Type Fuel – Design Selection.
12. Y. Soo, G.L. Hofman, J.S. Cheon, "Recrystallization and fission-gas-bubble swelling of U – Mo fuel," *Journal of Nuclear Materials,* **436**, 14–22 (2013)
13. A. Leenaers, S. van den Berghe, W. Renterghem, et al, "Irradiation behavior of ground U (Mo) fuel with and without Si added to the matrix," *Journal of Nuclear Materials,* **412**, 41–52 (2011)

14. A. Hanson and D. Diamond, "Calculation of Design Parameters for an Equilibrium LEU Core in the NBSR using a U7Mo Dispersion Fuel," No. BNL--105311-2014-IR, *Brookhaven National Laboratory* (2014)
15. N. Brown N and A. Cuadra, "Conversion Preliminary Safety Analysis Report for the NIST Research Reactor," No. BNL--107265-2015-IR, *Brookhaven National Laboratory*, (2015)
16. A. Hanson and D. Diamond, "A Neutronics Methodology for the NIST Research Reactor Based on MCNPX," No. BNL--95208-2011-CP, *Brookhaven National Laboratory*, (2011)
17. P. Kopetka, R.E. Williams, and J.M. Rowe. "NIST Liquid Hydrogen Cold Source," NISTIR 7352, *US Department of Commerce*, National Institute of Standards and Technology, 2006.